Available online at www.sciencedirect.com
SCIENCE DIRECT
Journal of Power Sources 153 (2006) 281–287
JOURNAL OF POWER SOURCES
www.elsevier.com/locate/jpowsour

Advanced materials for the 3D microbattery

D. Golodnitsky [a,b,*], V. Yufit [c], M. Nathan [c], I. Shechtman [a], T. Ripenbein [a,c], E. Strauss [a], S. Menkin [a], E. Peled [a]

[a] *School of Chemistry, Tel Aviv University, Tel Aviv 69978, Israel*
[b] *Wolfson Applied Materials Research Center, Tel Aviv University, Tel Aviv 69978, Israel*
[c] *Department of Physical Electronics, School of Electrical Engineering, Tel Aviv University, Tel Aviv 69978, Israel*

Available online 12 July 2005

Abstract

Out recent achievements in the development of three-dimensional (3D) thin film microbatteries on silicon and on microchannel plates (MCP) are presented. In such 3D microbatteries, the battery sandwich-like structure, including electrodes, electrolyte and current collectors, is deposited conformally on all available surfaces, thereby utilizing the dead volume of the substrate. Thin-film molybdenum oxysulfide and iron sulfide cathodes were deposited galvanostatically. XRD, XPS and TOF–SIMS characterizations indicated that the submicron thick MoO_yS_z films were amorphous, with the stoichiometry of the films varying with depth. Electrodeposited FeS_x films have an amorphous, network-like porous structure with nanosize particles. A special flow cell for conformal coating of the perforated substrates was designed. A Li/hybrid polymer electrolyte (HPE)/MoO_yS_z-on-Si 3D half cell ran at $i_d = i_{ch} = 10\ \mu A\ cm^{-2}$ and room temperature for 100 charge/discharge cycles with 0.1%/cycle capacity loss and 100% Faradaic efficiency. A 3D half cell on MCP exhibited 20 times higher capacity than that of a planar half cell with the same footprint.

Keywords: Thin-film cathode; Microbattery

1. Introduction

Miniature power sources are needed for a variety of applications, including implantable medical devices, remote sensors, miniature transmitters, "smart" cards, backup power for PC memory, and micro-electromechanical-system (MEMS) devices. A microbattery is defined as a solid-state electrochemical power source fabricated on the same scale (and sometimes substrate) as semiconductor circuitry and using the same type of processing techniques. A major advance in the integration of electronic and/or electromechanical devices with electrochemical power sources on the same chip was the development, started in the late 1980s of planar thin-film, solid-state, rechargeable, lithium and lithium-ion batteries by a group at Oak Ridge National Laboratories led by Bates [1]. A planar thin film battery is composed of successive sub-micron to several micron-thick layers of cathode ($LiCoO_2$ or $LiMn_2O_4$), lithium-phosphorous oxynitride (LIPON) electrolyte and a lithium or silicon tin oxynitride anode. The cathode and anode are typically formed by RF-magnetron sputtering, and the electrolyte by thermal evaporation or sputtering. The main drawback of planar cells implemented on different substrates is low current and low capacity, the latter directly proportional to the area and thickness of the electroactive layers. In order to increase battery capacity, we have recently developed methods of creating a 3D microbattery in a substrate perforated with high-aspect-ratio micro-holes or micro-channels [2]. In such a perforated substrate, one obtains an increase of more than an order of magnitude in the surface area available for active cathode and anode materials, over the original substrate footprint. The expected consequence is a similar order-of-magnitude increase in the capacity of the battery. It is clear that the geometrical area gain (AG) depends on the number of complete microchannels obtained by perforation and on the aspect ratio. The area gain is calculated according

* Corresponding author.
E-mail address: golod@post.tau.ac.il (D. Golodnitsky).

0378-7753/$ – see front matter © 2005 Elsevier B.V. All rights reserved.
doi:10.1016/j.jpowsour.2005.05.029

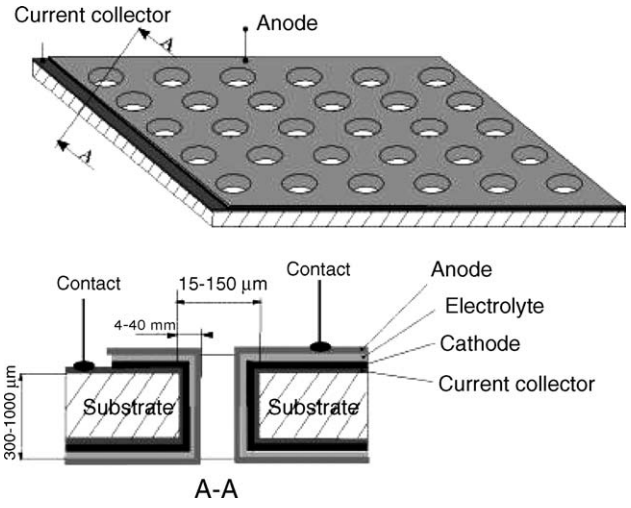

Fig. 1. Schematic presentation of the 3D microbattery.

the following equation:

$$\mathrm{AG} = \frac{\pi d}{(d+s)^2}\left(t - \frac{d}{2}\right) + 2 \quad (1)$$

where d is the microchannel diameter (μm), s the interhole spacing (μm), and t is the thickness of the substrate (μm).

For example, for a microchannel plate (MCP) substrate, built of many precision (soda-lime) glass capillary tubes fused together, the active-surface-area gain is ca. 25, when $d = 30$ μm, $s = 15$ μm, $t = 0.5$ mm.

In this contribution, the accent is on the development of a 3D-on-silicon microbattery, where the battery sandwich-like structure, including electrodes, electrolyte and current collectors, is deposited conformally on all the available top, bottom and internal hole surfaces of the perforated Si. The main idea was to use the dead volume of the chip and, by this means, to achieve a capacity gain of the battery. The schematic presentation of such a 3D-structure is shown in Fig. 1.

The development of a 3D-multilayered structure is clearly an extremely complex process. In addition to the different internal stresses of each material, special consideration must be given to interfacial phenomena. A typical battery formation process comprises seven different steps, each of which must be accomplished successfully:

1. Preparation of high-aspect-ratio perforated silicon, e.g. by inductively coupled plasma (ICP) etching (also known as DRIE).
2. Surface pretreatment of sidewalls.
3. Electroless deposition of a current collector.
4. Electrodeposition of a thin-film molybdenum sulfide or iron sulfide cathode.
5. Hybrid-polymer electrolyte coating.
6. Lithiation of graphite and filling the rest of each cavity with this anode material.
7. Charging of the cell with liquid electrolyte and packing.

The project is still very much in progress and, therefore, we present just our most recent results. Some data for a 3D microbattery built on MCPs will be shown as well.

2. Experimental

A Si substrate containing arrays of through-holes was prepared with the use of photolithography and DRIE. This substrate was a double side polished, (1 0 0), 440 μm thick, 3 in. silicon wafer. The wafer was coated on one side with about 10 μm of AZ-4562 photoresist, and arrays of square holes with a side dimension of 40 μm and inter-hole spacing of about 10 μm were defined. The sequence of photolithography steps included:

1. Dehydration bake of wafers after cleaning for 2 min at 110 °C on a hot plate.
2. Dispensing photoresist and spinning at about 1400 rpm for 30 s.
3. Solvent removal bake at 110 °C for 1 min on a hot plate.
4. Exposure for between 17 and 22 s in a mask aligner.
5. Development for 4–6 min in an AZ-726 developer.
6. Hard bake at 110 °C for 3 min on the hot plate.
7. Hole etching in a Plasma-Therm SLR 770 DRIE system using a standard Bosch process.

Thin film, nominally MoS_2 cathodes were prepared electrochemically in an aqueous 0.028 M solution of tetrathiomolybdate (MoS_4^{2-}) ions according to a procedure described elsewhere [3]. The iron sulfide films were electrodeposited galvanostatically on a nickel or nickel-coated silicon substrate with the use of a conventional two-electrode cell with a carbon counter electrode. The electroplating bath contained: 0.01 M $Fe_2(SO_4)_3$, 0.3 M $Na_2S_2O_3$, 0.03 M sodium citrate and 0.1 g L^{-1} sodium dodecylsulfate [4]. The temperature of the bath was 50 °C, $i = 1$–10 mA cm^{-2}, pH 3.5–4.0 was adjusted by the addition of H_2SO_4. All solutions were prepared from analytical-grade chemicals dissolved in Millipore water (>18 MΩ cm). The thickness of the deposits was measured by a Dectak 3 profilometer.

A JSM-6300 scanning microscope (Jeol Co.) equipped with a Link elemental analyzer and a silicon detector was used to study surface morphology. X-ray diffraction data were obtained with the use of a θ–θ Scintag powder diffractometer equipped with a Cu Kα source and a liquid-nitrogen germanium solid-state detector. X-ray photoelectron spectroscopy (XPS) tests of as-deposited films were performed with a monochromatic Al Kα source (1486.6 eV) in ultra-high vacuum (2.5×10^{-10} Torr) with a 5600 Multi-Technique System (Physical Electronics Inc., USA). Depth profiles were obtained by argon ion sputtering, at a sputtering rate of 0.5 nm min^{-1} based on a SiO_2/Si sample. TOF–SIMS tests were conducted with the use of TRIFT II (Physical Electronics Inc., USA) under the following operating conditions: primary ions, In^+ and a dc sputtering rate, 2 Å s^{-1} based on SiO_2.

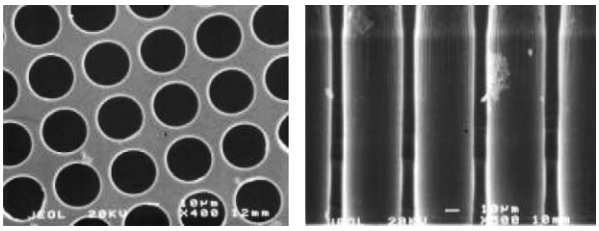

Fig. 2. Plane and cross-sectional SEM micrographs of the perforated silicon.

The electrochemical cells studied comprised a lithium anode, hybrid (HPE) or composite solid polymer electrolyte (CPE), and a MoS_2 cathode. For the lithium-ion cells, chemically [5] or electrochemically prepared lithiated graphite was used as the anode.

3. Results and discussion

Fig. 2 depicts the planar and cross-sectional SEM images of the perforated silicon substrate with a high aspect ratio (7.5:1) micro-holes. As can be seen from the image, cylindrical channels of about 40 μm diameter and penetrating the entire thickness of the wafer are obtained by ICP etching under appropriate operating conditions. A conventional etch is used until just before the buried oxide-silicon interface is reached, followed by a highly polymerizing etch of the buried oxide, thus avoiding the scalloping of the sidewalls and the undercutting of the silicon on the SiO_2/Si and Si/photoresist interfaces.

The AFM images (Fig. 3) of the silicon wafer after ICP perforation show a significant difference in the surface morphology inside a micro-hole compared to that of a flat area. The flat area is rather smooth, with a mean roughness of about 10 nm. The roughness inside a hole varies from 16 to 100 nm. A number of degreasing and etching solutions, like acetone, ethanol, weakly alkaline solution and mixtures of HF, HNO_3 and CH_3COOH were tested in an effort to smooth the internal sidewall roughness and bring it closer to that of a flat area, and in order to get layers of current collector and cathode that adhere well to Si. We found that one of the promising ways to provide good Ni–Si adhesion is by metal (Pd)-assisted chemical preparation of nano-porous silicon, carried out in a solution of 50 HF:20 C_2H_5OH:30

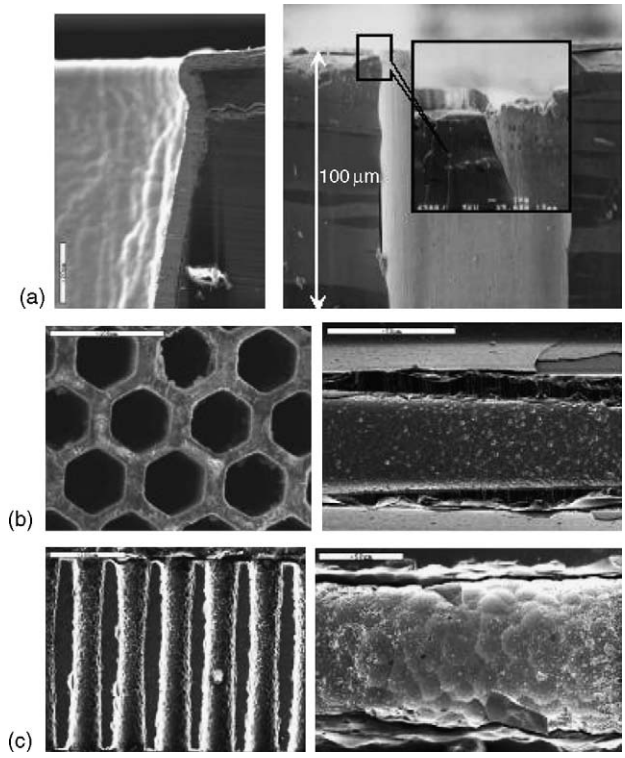

Fig. 4. SEM micrographs of the perforated silicon, MCP and Foturan substrates conformally coated by a nickel current collector.

H_2O_2 (%, v/v). This process creates pits with a depth that increases with etching time. The pore size depends on the thickness of the sacrificial metal layer.

An electroless method, which is known to provide conformal coatings, was used to deposit the nickel current collector on all available top and bottom surfaces of the perforated silicon wafer and inside the holes.

Prior to electroless plating, pretreated silicon samples were catalyzed by the deposition of palladium, usually in a solution of $PdCl_2$, HCl and HF. This was followed by a multi-step washing in deionized water.

The electroless plating was performed in a solution of $NiSO_4$, $Na_2H_2PO_2$ as a reducing agent, and sodium citrate as a complexing agent and buffer. From the SEM micrographs (Fig. 4a), it is clear that the deposition, carried out at 80 °C, pH 8–9 for 5–10 min yielded a uniform 2–4 μm thick nickel

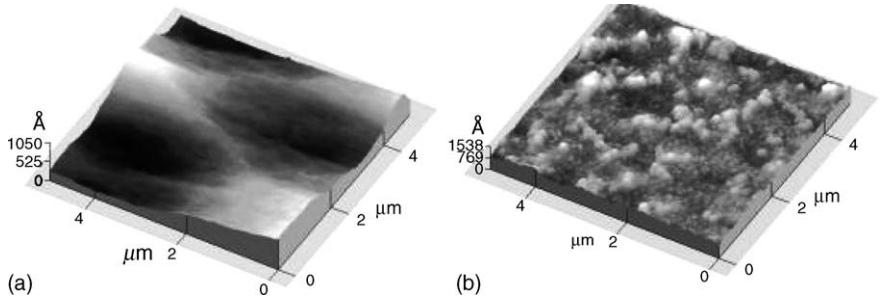

Fig. 3. AFM images of the internal channel surface and flat areas of the perforated silicon substrate.

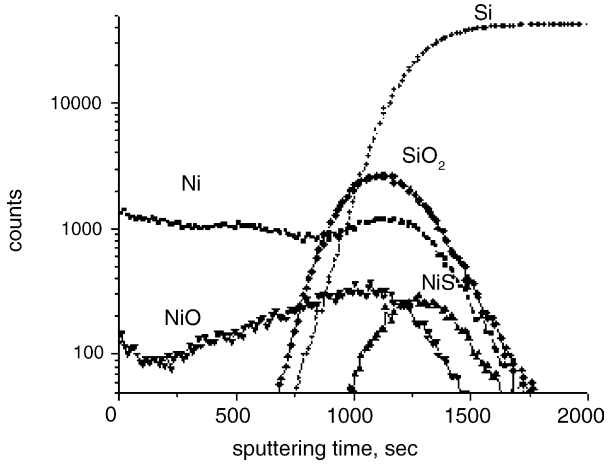

Fig. 5. TOF–SIMS depth profile of a silicon substrate coated by a nickel layer after thermal treatment at 200 °C.

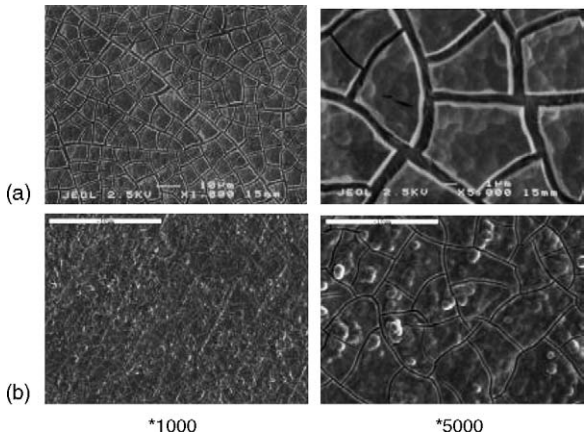

Fig. 6. SEM micrographs of the molybdenum oxysulfide cathode obtained by electrodeposition under direct (a: 10 mA cm^{-2}) and pulse current (b: current amplitude, 10 mA cm^{-2}, cathodic/anodic pulse current ratio = 500:100 ms) conditions.

layer both inside the hole and on the flat area. A continuous nickel layer and complete coverage of the trough holes are achieved. The average roughness of the nickel coating is about 150 nm. When trying to deposit the nickel current collector on the MCP and Foruran substrates, we were faced with a severe problem of extremely poor adhesion. Foturan is a photosensitive glass, in which hole arrays are formed by photolithography and etching. The composition of MCP and Foturan materials is close to that of soda-lime glass (w/w, %): SiO_2 (72.8), Na_2O (13.7), CaO (8.8), MgO (4.0), Fe_2O_3 (0.12), Al_2O_3 (0.1). Both glass substrates were degreased in hot cyclohexane to increase the wettability of the surface, cleaned in boiling Piranha solution (H_2SO_4:H_2O_2) for 10 min, dipped in 1 M HCl to dissolve the remaining CaF_2 and MgF_2 and subsequently etched in 1 M NaOH. As with the perforated silicon substrate, conformal and highly adherent deposits of the nickel current collector with complete coverage of the microchannels was achieved under appropriate operating conditions (Fig. 4b and c). Thermal treatment (200 °C for 4 min in an argon atmosphere) of the Ni-coated samples improved adhesion still further. This was due to nickel diffusion into the Si bulk and formation of about a 100 nm thick layer of nickel silicide on the interface of the substrate and current collector, as shown by the TOF–SIMS depth profile (Fig. 5).

At present, the main techniques for preparing thin-film cathodes include chemical-vapor deposition (CVD), sputtering, spray pyrolysis and evaporation. Some of these processes are typically carried out at high temperatures and need very expensive equipment. We developed here an inexpensive and relatively simple electrodeposition method for preparing low-cost and low-toxicity molybdenum and iron sulfide thin cathode layers. The molybdenum sulfide cathodes were deposited from a freshly prepared tetrathiomolybdate (formed by chemical reaction in a solution of Na_2MoO_4 and Na_2S. The detailed procedure is described elsewhere [6]. A highly adherent, homogeneous, compact film about 300 nm thick can be deposited on nickel-coated silicon and glass substrates. An increase in the deposition time or current density is followed by the formation of cracks, which may be responsible for film peeling, and inability to deposit thicker cathodes. It seems likely that these cracks are caused by high internal stresses that develop during deposition. The deposits become smoother and the width of the cracks is lowered by pulse current deposition (Fig. 6). The EDS analysis indicated a large atomic surface concentration of oxygen. A powder XRD pattern of as-deposited cathode films did not show crystallographic peaks belonging to molybdenum sulfide or molybdenum oxide. This may indicate that the electrodeposited film is mainly amorphous.

In order to obtain more precise information on the composition of the electrodeposited cathode material, high-resolution XPS measurements were carried out at different sputtering times. Analyses of the elemental depth profile reveal that molybdenum oxides dominate on the surface of the as-deposited cathode, while in the bulk, the concentrations of Mo–S and Mo–O bond-containing compounds are comparable [7]. In order to determine whether the cathode is composed of a mixture of molybdenum oxide and sulfide, or if there is formation of a new compound like molybdenum oxysulfide, high-resolution TOF–SIMS tests were carried out. A variety of oxygen- and sulfur-containing molybdenum fragments, like MoO_2, MoS, MoS_2, MoO_4 were found in the cathode. A distinctive feature of the spectra (Fig. 7) is the presence of the polyion clusters containing both oxygen and sulfur, like MoOS, MoO_2S and MoS_2O. These species were found both on the surface and in the bulk of the electrode and in our opinion are of primary importance, as their appearance unambiguously indicates formation of molybdenum oxysulfide during electrodeposition. In agreement with the XPS data the concentration of sulfur containing fragments, calculated from the TOF–SIMS spectra, increases with sputtering time. After 11 min of sputtering, for example, which provides close

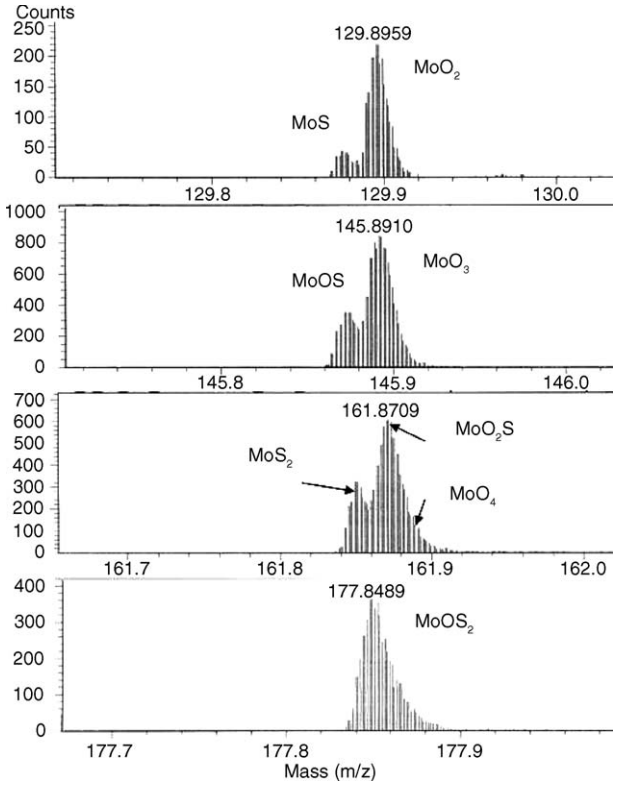

Fig. 7. TOF–SIMS spectra of molybdenum oxysulfide cathode.

to 100 nm film depth, MoS_2 and MoO_2S species predominate [6].

The galvanostatic electrodeposition of FeS was carried out on a nickel current collector. Black, smooth 0.3–1.5 μm thick deposits were obtained at current densities of 1–10 mA cm^{-2} [4]. Iron sulfide deposits at low current density are made up of closely packed units of several square micron areas. Each unit has a porous network-like structure. Grain size appears to be inversely proportional to deposition time. The films were X-ray transparent, indicating amorphous structure. From the high resolution XPS analysis, it was deduced that there are at least three iron sulfide derivatives in the deposit. The first one is FeS_2, the second is iron monosulfide and the third, a non-stoichiometric FeS_{1+x} compound. The atomic concentration ratio: $FeS_2/(FeS + FeS_{1+x})$ is 1:4, and does not change even after 12 min of sputtering.

A flow-cell was designed to promote the conformal coating of the perforated substrates by a thin-film cathode. Electrodeposition with a laminar flow-rate of electrolyte of between 100 and 200 mL min^{-1} resulted in an unbroken cathode film of uniform thickness along the total vertical extent of the cylindrical microchannels. It is noteworthy, that the structure of the cathode material inside the hole is the same as on the flat area (Fig. 8).

We recently carried out intensive studies of hybrid polymer electrolytes (HPE) for the Li/pyrite battery [8]. A commercially available PVDF-2801 copolymer (Kynar) was been chosen as binder, and fumed silica, as filler for the

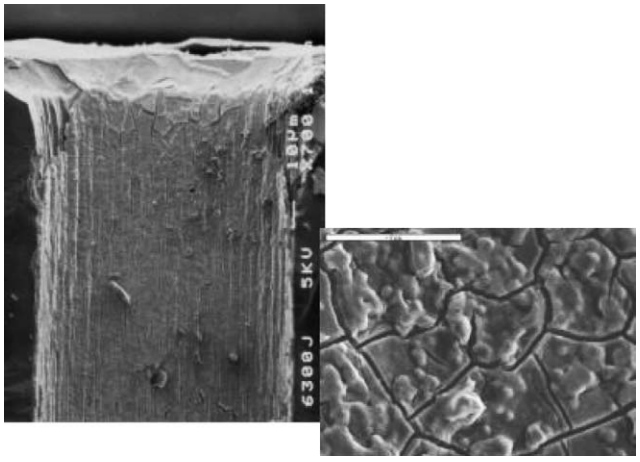

Fig. 8. Cross-sectional SEM micrographs of a silicon microchannel coated by a molybdenum oxysulfide cathode.

polymer membrane, similar to the Bellcore process. The membranes were prepared by the doctor-blade technique. Ionic conductivity of a 1–3 mS cm^{-1} at room temperature (RT) was achieved for HPEs, with a membrane soaked either in tetraglyme or EC:DMC-based electrolyte with LiImide salt. The interfacial lithium/HPE resistance (R_{SEI}) of 6–10 Ω cm^{-2} was stable for 3000 h. In this work, successive steps of spin coating and vacuum were used to insert the membrane into the perforated substrates. SEM images (Fig. 9) show conformal coating of the microchannels of the perforated silicon, Foturan and glass capillary arrays. The thickness of the membrane and its morphology depend on the type of solvent, pore former (PC or PEG), percent of solids in the casting slurry and drying conditions. The membranes cast from cyclopentanone were transparent or slightly translucent with smooth homogeneous surface and bulk. The membrane cast from acetone has less uniform morphology, with surface irregularities and sometimes trapped air bubbles. This is due to the extremely fast evaporation of the solvent.

The preparation of lithiated graphite is still in the initial experimental stage. For the first prototypes of the 3D microbatteries, mesocarbon microbeads (MCMB), and expanded graphite of 1–6 μm particle size were used as lithium intercalation host materials. Electrochemical and chemical procedures via the formation of lithium–naphthalene-1-methoxybutane (Li–NM) complex [5] are under development. A graphite intercalation compound (composition: $LiC_{8.5}$), corresponding to the mixed first and second stages of lithium-to-graphite intercalation, was obtained. As with the HPE membrane, spin coating and vacuum steps were used to fill the remaining cylindrical cavities of the microchannels with anode material.

Initially, to check the feasibility of thin-film cathodes, lithium and Li-ion/hybrid polymer electrolyte/MoO_xS_y on-silicon batteries in planar configuration were assembled and cycled on a 16-bit Maccor 2000 Battery Tester. The sloping character of the curves (Fig. 10a) is typical of lithium insertion/de-insertion into a single-phase host

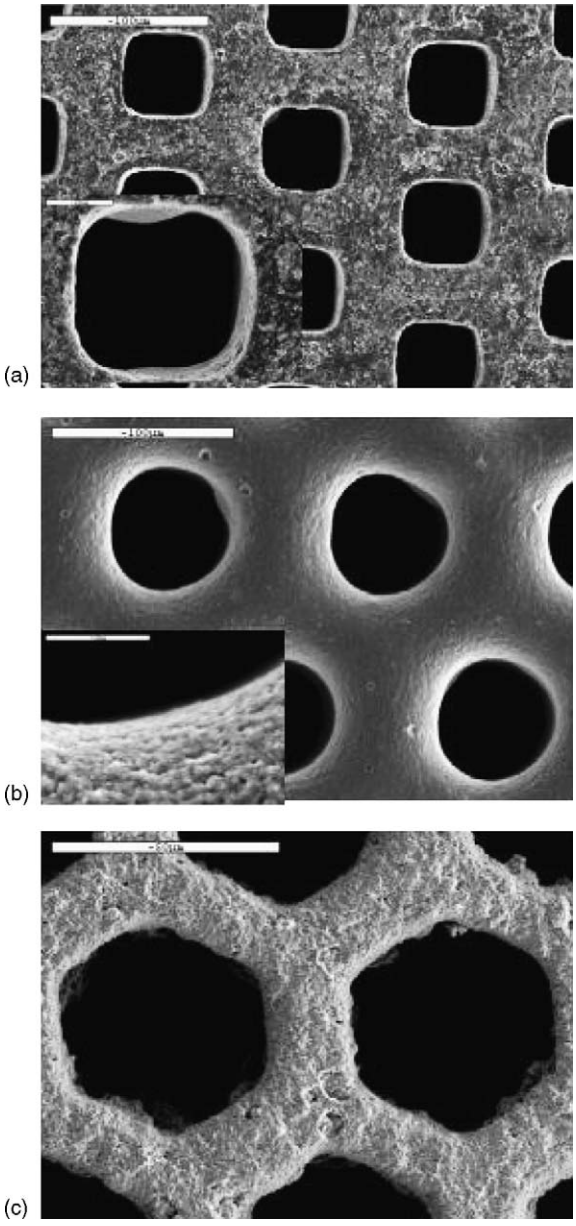

Fig. 9. SEM micrographs of the perforated Si (a), Foturan (b) and MCP (c) substrates, coated by nickel, molybdenum oxysulfide cathode and hybrid polymer electrolyte membrane.

material according to reaction (2).

$$MoO_xS_y + nLi^+ + ne \rightarrow Li_n{\cdot}MoO_xS_y \quad (2)$$

We would like to emphasize that up to a 10-fold increase in the current density (from 10 to 100 μA cm^{-2}) did not influence either the shape of the curves or the degradation rate. The first-cycle utilization of the cathode-active material approached 85%. Lithium and Li-ion/HPE/MoO_yS_z cells ran over 1000 successive cycles with 0.02–0.05%/cycle capacity loss and 100% Faradaic efficiency (Fig. 10b). No self-discharge was detected in any of the Li-ion/MoO_yS_z cells under investigation. It was also found that slow overdischarge to 0.2 V does not affect the subsequent cycling behavior of the Li/MoO_xS_y

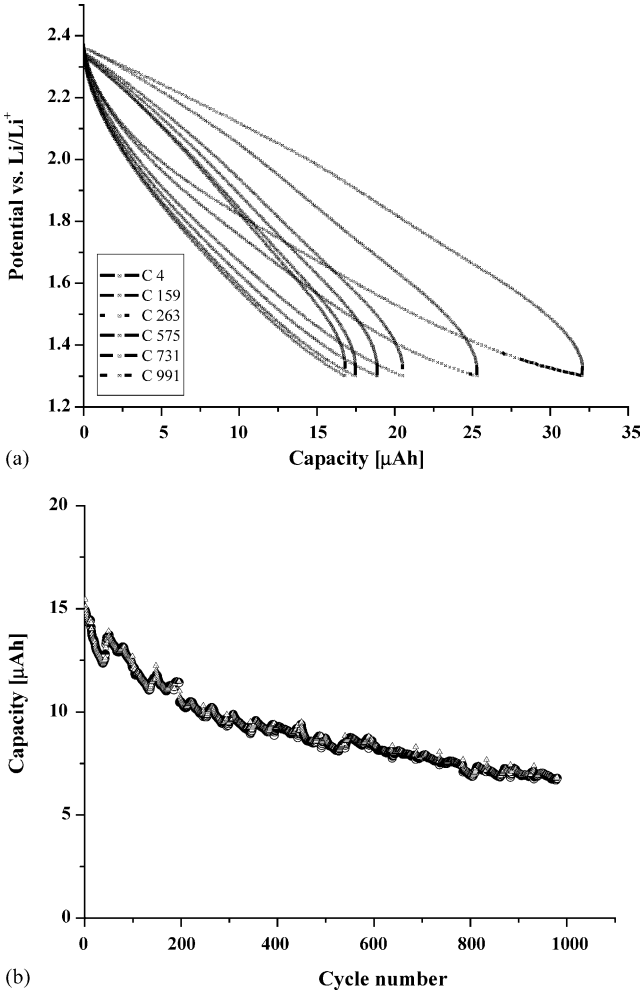

Fig. 10. (a) Typical charge–discharge curves of a room temperature Li-ion/$LiAsF_6$ EC:DEC (1:2) HPE/MoO_yS_z cell with a cathode deposited on a nickel-coated planar silicon substrate. Cycling conditions: $V_{cut\text{-}off}$ = 1.3–2.4 V; $i_{dis} = i_{ch}$ = 10 μA cm^{-2}. (b). Long-term cycling of the same cell. Cycling conditions: $V_{cut\text{-}off}$ = 1.3–2.4 V; $i_{dis} = i_{ch}$ = 100 μA cm^{-2}.

batteries. A Li/composite polymer electrolyte/FeS_{2-x} cell ran at $i_d = i_{ch}$ = 50 μA cm^{-2} (c/1 rate) and 125 °C for over 650 charge/discharge cycles with 0.06% degradation rate [4].

Finally, a number of 3D-on-Si half cells were assembled and cycled. The cell comprised a perforated Si sample coated by a Ni current collector and MoO_xS_y cathode. The microchannels were completely filled by the HPE. This sample was placed between two planar lithium anodes in a coin cell 2032. The sloping character of the discharge curves is similar to that of the plane cell configuration (Fig. 11a). The 3D-half cell ran over 100 reversible cycles with about 1%/cycle capacity loss and, at time of writing, is still running (Fig. 11b). Another 3D Li half cell on glass capillary arrays with cylindrical channels continuously filled by hybrid polymer electrolyte was recently assembled and so far has run over 10 reversible cycles. We would like to emphasize that capacity gain correlated completely with the geometrical area gain

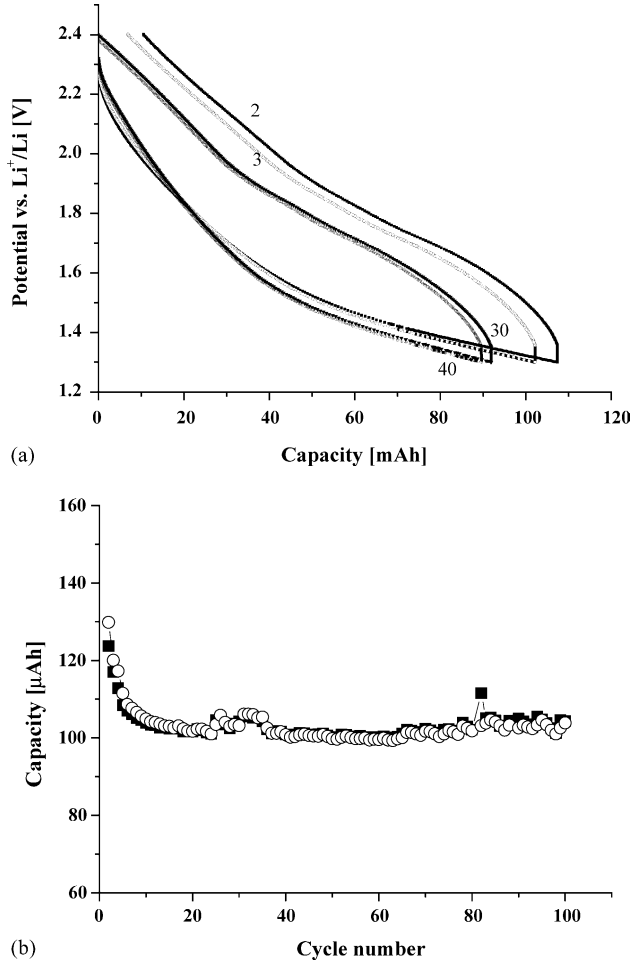

Fig. 11. (a) Typical charge–discharge curves of a 3D Li/LiAsF$_6$ EC:DEC (1:2) HPE/MoO$_y$S$_z$ half cell. Cycling conditions: $V_{cut\text{-}off} = 1.3$–2.4 V; $i_{dis} = i_{ch} = 10\,\mu A\,cm^{-2}$, (b) capacity vs. number of cycles of the 3D half cell.

of the MCP (Eq. (1)). The reversible 1.0 mAh cm^{-2} battery capacity is about 20 times that of a planar battery.

4. Summary

Three-dimensional perforated Si substrates with high-aspect ratio vertical channels have been prepared using DRIE. A highly-adherent Ni current collector has been conformally deposited on the perforated Si, microchannel plate glass capillary arrays and Foturan substrates. Submicron to several micronthick electrochemically deposited molybdenum oxysulfides and iron sulfides can serve as good cathodes in thin-film planar and 3D Li and Li-ion cells. These are advantageous in their simple and inexpensive preparation method and are conformal to the shape of a substrate. A lithium and Li-ion/HPE/MoO$_x$S$_y$-on-Si planar cell ran at $i_d = i_{ch} = 100\,\mu A\,cm^{-2}$ and RT for 1000 charge/discharge cycles with 0.02–0.06%/cycle capacity loss and 100% Faradaic efficiency. Similar results were obtained for cells with FeS$_x$ cathodes. Preliminary tests of the 3D half cells were carried out. The capacity gain of the 3D thin-film microbattery formed on an MCP substrate correlates extremely well with the geometrical area gain provided by the capillaries.

Acknowledgements

We would like to especially thank Dr. L. Burstein, Dr. Yu. Rozenberg, Dr. A. Gladkich and Dr. Z. Barkai of the Wolfson Applied Materials Research Center for conducting the XPS, XRD, SEM, TOF–SIMS and AFM measurements. We express our gratitude to the Government of Israel, RAMOT (University Authority for Applied Research and Industrial Development Ltd.), and to USAF (Contract No. F61775-01-WE020, FeS cathodes), for partial support of this project.

References

[1] J.B. Bates, N.J. Dudney, G.R. Gruzalski, et al., J. Power Sources 43 (1993) 127.
[2] M. Nathan, E. Peled, D. Haronian, Microelectrochemical Cell, US Patent No. 6,197,450.
[3] E.A. Ponomarev, M. Neumann-Spallart, G. Hodes, C. Levy-Clement, Thin-Solid Films 280 (1996) 86.
[4] V. Yufit, K. Freedman, M. Nathan, L. Burstein, D. Golodnitsky, E. Peled, Electrochim. Acta, 2003.
[5] S. Hashikawa, et al., Z. Naturforsch. 57a (2002) 857–862.
[6] D. Golodnitsky, M. Nathan, V. Yufit, E. Strauss, K. Freedman, L. Burstein, A. Gladkich, E. Peled, Solid State Ionics, submitted for publication.
[7] V. Yufit, M. Nathan, D. Golodnitsky, E. Peled, J. Power Sources (2003) 169–173.
[8] G. Ardel, D. Golodnitsky, E. Peled, G.B. Appetecchi, P. Romagnoli, B. Scrosati, J. Power Sources 110 (2002) 152–162.